

Analyzing the two-dimensional doped Hubbard model with the Worldvolume HMC method[†]

Masafumi Fukuma^a and Yusuke Namekawa^{b,*}

^a*Department of Physics, Kyoto University, Kyoto 606-8502, Japan*

^b*Department of Computer Science, Fukuyama University, Hiroshima 729-0292, Japan*

E-mail: fukuma@gauge.scphys.kyoto-u.ac.jp, namekawa@fukuyama-u.ac.jp

We apply the Worldvolume Hybrid Monte Carlo (WV-HMC) method [arXiv:2012.08468] to the two-dimensional Hubbard model, which is known to suffer from a severe sign problem when the system is doped (away from half filling). We show that the method predicts physical observables with controlled statistical errors on an 8×8 lattice at temperature $T/t = 1/6.4 \approx 0.156$ and interaction strength $U/t = 8.0$ (t is the hopping amplitude), for which the standard determinant quantum Monte Carlo fails.

The 42nd International Symposium on Lattice Field Theory (LATTICE2025)

2-8 November 2025

Tata Institute of Fundamental Research, Mumbai, India

[†]Report No.: KUNS-3102

*Speaker

1. Introduction

The numerical sign problem has long been a major obstacle to first-principle computations of various important physical systems, such as finite-density QCD, strongly correlated electron systems, and real-time dynamics of quantum many-body systems. Among them, the Hubbard model has a unique position in the research area of the sign problem, not only because of its importance in condensed-matter physics, but also because of its similarity in the mathematical structure to finite-density QCD.

For the Hubbard model, the standard quantum Monte Carlo method suffers from the severe sign problem when the system is doped (away from half filling), and the model has been extensively studied using diverse methods, ranging from Variational Monte Carlo [1–4] and Constrained-Path Auxiliary-Field Quantum Monte Carlo [5, 6], to rather new approaches such as the Lefschetz thimble method [7–12], the tempered Lefschetz thimble (TLT) method [13], tensor renormalization group [14, 15], complex-valued neural networks [16], constant path-integral contour shifts [17], and normalizing flows [18].

For the last fifteen years, there has been an academic trend to construct a versatile solution to the sign problem, and various methods have been proposed. Among them, the Worldvolume Hybrid Monte Carlo (WV-HMC) [19] (see also Refs. [20–25]) was proposed as a reliable and low-cost algorithm that resolves the sign problem. This is based on the idea of the thimble method but is free from the ergodicity problem inherent in thimble approaches by considering a continuum union of deformed integration surfaces. In this paper, based on Refs. [24, 25], we report its application to the two-dimensional doped Hubbard model. We particularly demonstrate that the method predicts physical observables with controlled statistical errors on an 8×8 lattice at temperature $T/t = 1/6.4 \approx 0.156$ and interaction strength $U/t = 8.0$ (t is the hopping amplitude), for which the standard determinant quantum Monte Carlo fails.

2. WV-HMC method via embedding GT-HMC

We here give a brief review on the basics of WV-HMC. Let $x = (x^a) \in \mathbb{R}^N$ be a variable of N degrees of freedom. Our aim is to numerically evaluate an observable $O(x)$ with a complex action $S(x)$:

$$\langle O \rangle \equiv \frac{\int_{\mathbb{R}^N} dx e^{-S(x)} O(x)}{\int_{\mathbb{R}^N} dx e^{-S(x)}} \quad \left(dx = dx^1 \wedge \cdots \wedge dx^N \equiv \prod_{a=1}^N dx^a \right). \quad (2.1)$$

Following the Lefschetz thimble method [26–33], we complexify $x = (x^a)$ to $z = (z^i)$ ($i = 1, \dots, N$), and deform the integration surface from $\Sigma_0 \equiv \mathbb{R}^N$ into Σ within the complexified space \mathbb{C}^N . This deformation is governed by the anti-holomorphic flow:

$$\dot{z} = \overline{\partial S(z)} \quad \text{with } z|_{t=0} = x, \quad (2.2)$$

where $\dot{z} = \partial z / \partial t$ (t : the deformation parameter referred to as the *flow time*). Writing the solution by $z = z(t, x)$, the deformed surface at flow time t is given by $\Sigma = \Sigma_t \equiv \{z(t, x) \mid x \in \Sigma_0\}$. Cauchy's

theorem guarantees that the integrals do not change under the flow, so that Eq. (2.1) is written as

$$\langle O \rangle = \frac{\int_{\Sigma_t} dz e^{-S(z)} O(z)}{\int_{\Sigma_t} dz e^{-S(z)}} \quad (dz = dz^1 \wedge \cdots \wedge dz^N). \quad (2.3)$$

At large flow times t , Σ_t approaches the Lefschetz thimbles (constant $\text{Im } S$ surfaces), which suppresses the phase fluctuation from $e^{-i\text{Im } S(z)}$. However, this large t introduces ergodicity issues: zeros of $e^{-S(z)}$ appear on Σ_t , acting as infinitely high potential barriers for Markov chain updates. The generalized thimble (GT) method [33] uses an intermediate t to balance sign suppression and ergodicity. However, detailed studies show that sign suppression generally requires Σ_t to cross zeros [13], leaving the fundamental tension unresolved.

The tempered Lefschetz thimble (TLT) method [34] resolves this tension by treating t as a dynamical variable. However, TLT incurs a high computational cost because it requires computing the deformation Jacobian at every replica exchange. The Worldvolume Hybrid Monte Carlo (WV-HMC) method [19] (see also Refs. [20–25]) eliminates this bottleneck. This can be regarded as a continuous version of the TLT method and introduced as follows.

Since both the numerator and the denominator in Eq. (2.3) are independent of t (due to Cauchy's theorem), we can take averages over t separately with an arbitrary common weight $e^{-W(t)}$ [19]:

$$\langle O \rangle = \frac{\int dt e^{-W(t)} \int_{\Sigma_t} dz e^{-S(z)} O(z)}{\int dt e^{-W(t)} \int_{\Sigma_t} dz e^{-S(z)}}. \quad (2.4)$$

This takes the form of a ratio of reweighted averages on the *worldvolume* \mathcal{R} ,

$$\mathcal{R} \equiv \bigcup_t \Sigma_t = \{z(t, x) \mid t \in \mathbb{R}, x \in \mathbb{R}^N\}, \quad (2.5)$$

as

$$\langle O \rangle = \frac{\langle \mathcal{F}_{\mathcal{R}}(z) O(z) \rangle_{\mathcal{R}}}{\langle \mathcal{F}_{\mathcal{R}}(z) \rangle_{\mathcal{R}}}, \quad (2.6)$$

$$\langle g(z) \rangle_{\mathcal{R}} \equiv \frac{\int_{\mathcal{R}} |dz|_{\mathcal{R}} e^{-\text{Re } S(z) - W(t)} g(z)}{\int_{\mathcal{R}} |dz|_{\mathcal{R}} e^{-\text{Re } S(z) - W(t)}}. \quad (2.7)$$

Here, $|dz|_{\mathcal{R}}$ is the invariant measure on \mathcal{R} , and $\mathcal{F}_{\mathcal{R}}(z) \equiv dt dz e^{-i\text{Im } S(z)} / |dz|_{\mathcal{R}}$ is the associated reweighting factor. The extent of the worldvolume \mathcal{R} in the t -direction can be restricted within a finite interval $[T_0, T_1]$ by tuning the function $W(t)$, which we take as follows [21]:

$$W(t) = \begin{cases} -\gamma(t - T_0) + c_0 (e^{(t-T_0)^2/2d_0^2} - 1) & \text{for } t < T_0 \\ -\gamma(t - T_0) & \text{for } T_0 \leq t \leq T_1 \\ -\gamma(t - T_0) + c_1 (e^{(t-T_1)^2/2d_1^2} - 1) & \text{for } t > T_1. \end{cases} \quad (2.8)$$

The reweighted average $\langle g(z) \rangle_{\mathcal{R}}$ can be further rewritten as a phase-space integral over the tangent bundle of \mathcal{R} ,

$$T\mathcal{R} = \{(z, \pi) \mid z \in \mathcal{R}, \pi \in T_z \mathcal{R}\}, \quad (2.9)$$

as

$$\langle g(z) \rangle = \frac{\int_{T\mathcal{R}} d\Omega_{\mathcal{R}} e^{-H(z,\pi)} g(z)}{\int_{T\mathcal{R}} d\Omega_{\mathcal{R}} e^{-H(z,\pi)}}. \quad (2.10)$$

Here, $d\Omega_{\mathcal{R}} \equiv \omega_{\mathcal{R}}^{N+1}/(N+1)!$ is the symplectic volume form constructed from the symplectic 2-form $\omega_{\mathcal{R}} = \text{Re}(d\pi^\dagger \wedge dz)$, and $H(z, \pi) = (1/2)\pi^\dagger \pi + \text{Re} S(z) + W(t(z))$.¹ The distribution function $\propto e^{-H(z,\pi)}$ can be generated using the HMC algorithm with constrained molecular dynamics such as RATTLE [35]. See Refs. [19, 21, 22] for details.

An HMC algorithm for the GT method [which we refer to as the *generalized thimble HMC* (GT-HMC)] can be introduced similarly [36, 37] (see also Ref. [21]) as a sampling on the tangent bundle of Σ , $T\Sigma = \{(z, \pi) \mid z \in \Sigma, \pi \in T_z \Sigma\}$, from the distribution $\propto e^{-H(z,\pi)}$ with the Hamiltonian $H(z, \pi) = (1/2)\pi^\dagger \pi + \text{Re} S(z)$. While GT-HMC alone suffers from ergodicity issues, embedding it as a subprocess within WV-HMC strongly enhances global sampling, particularly when the world-volume is a thin layer [25].

3. The Hubbard model

The Hubbard model on a d -dimensional spatial lattice is defined by the following Hamiltonian (including the chemical potential term):

$$\begin{aligned} \hat{H}_\mu^{\text{org}} &= \hat{H} - \mu \hat{N} \\ &\equiv - \sum_{\mathbf{x}, \mathbf{y}} t_{\mathbf{xy}} \sum_{\sigma=\uparrow, \downarrow} c_{\mathbf{x}, \sigma}^\dagger c_{\mathbf{y}, \sigma} + U \sum_{\mathbf{x}} n_{\mathbf{x}, \uparrow} n_{\mathbf{x}, \downarrow} - \mu \sum_{\mathbf{x}} (n_{\mathbf{x}, \uparrow} + n_{\mathbf{x}, \downarrow}). \end{aligned} \quad (3.1)$$

Here, $c_{\mathbf{x}, \sigma}$ and $c_{\mathbf{x}, \sigma}^\dagger$ denote the annihilation and creation operators, respectively, of an electron with spin σ ($=\uparrow, \downarrow$) at site $\mathbf{x} = (x_i)$ ($i = 1, \dots, d$), and $n_{\mathbf{x}, \sigma} \equiv c_{\mathbf{x}, \sigma}^\dagger c_{\mathbf{x}, \sigma}$. $t = (t_{\mathbf{xy}})$ is the hopping matrix, where $t_{\mathbf{xy}} = t$ (> 0) if \mathbf{x} and \mathbf{y} are nearest neighbors, and $t_{\mathbf{xy}} = 0$ otherwise. U is the on-site repulsion strength, and μ is the chemical potential associated with the number operator $\hat{N} = \sum_{\mathbf{x}} \sum_{\sigma} n_{\mathbf{x}, \sigma}$. We assume that the model is defined on a periodic, bipartite square lattice of linear size L_s , so that the spatial volume is given by $V_d \equiv L_s^d$.

We perform a particle-hole transformation on the down-spin component and write

$$a_{\mathbf{x}} \equiv c_{\mathbf{x}\uparrow}, \quad b_{\mathbf{x}} \equiv (-1)^{\mathbf{x}} c_{\mathbf{x}\downarrow}^\dagger, \quad (3.2)$$

where $(-1)^{\mathbf{x}} \equiv (-1)^{\sum_i x_i}$ denotes the parity of site \mathbf{x} . Under this transformation, the Hamiltonian (3.1) becomes (up to an additive constant $-\mu V_d$):

$$\hat{H}_\mu \equiv \hat{H}_\mu^{\text{org}} - \mu V_d = - \sum_{\mathbf{x}, \mathbf{y}} t_{\mathbf{xy}} (a_{\mathbf{x}}^\dagger a_{\mathbf{y}} + b_{\mathbf{x}}^\dagger b_{\mathbf{y}}) + \frac{U}{2} \sum_{\mathbf{x}} (n_{\mathbf{x}}^a - n_{\mathbf{x}}^b)^2 - \tilde{\mu} \sum_{\mathbf{x}} (n_{\mathbf{x}}^a - n_{\mathbf{x}}^b), \quad (3.3)$$

where $n_{\mathbf{x}}^a \equiv a_{\mathbf{x}}^\dagger a_{\mathbf{x}}$ and $n_{\mathbf{x}}^b \equiv b_{\mathbf{x}}^\dagger b_{\mathbf{x}}$, and the shifted chemical potential is defined as

$$\tilde{\mu} \equiv \mu - \frac{U}{2}. \quad (3.4)$$

¹ $t(z)$ returns the flow time t for configuration $z = z(t, x)$.

The point $\mu = U/2$ (i.e., $\tilde{\mu} = 0$) corresponds to half filling, where $\langle n_{\mathbf{x},\uparrow} + n_{\mathbf{x},\downarrow} \rangle = 1$ (i.e., $\langle n_{\mathbf{x}}^a - n_{\mathbf{x}}^b \rangle = 0$).

Following Ref. [38], we introduce the redundant parameter α ($0 \leq \alpha \leq 1$) as²

$$(n_{\mathbf{x}}^a - n_{\mathbf{x}}^b)^2 = \alpha(n_{\mathbf{x}}^a - n_{\mathbf{x}}^b)^2 - (1 - \alpha)(n_{\mathbf{x}}^a + n_{\mathbf{x}}^b - 1)^2 + 1 - \alpha. \quad (3.5)$$

We then complete the square by using two auxiliary variables (Hubbard-Stratonovich variables):

$$\begin{aligned} & e^{-(\alpha \epsilon U/2)(n^a - n^b)^2 + ((1 - \alpha) \epsilon U/2)(n^a + n^b - 1)^2 - (1 - \alpha) \epsilon U/2} \\ &= \int dA dB e^{-(1/2)(A^2 + B^2)} e^{[ic_0 A + c_1 B - c_1^2] n^a} e^{[-ic_0 A + c_1 B - c_1^2] n^b} \end{aligned} \quad (3.6)$$

with $c_0 \equiv \sqrt{\alpha \epsilon U}$ and $c_1 \equiv \sqrt{(1 - \alpha) \epsilon U}$. We decompose the inverse temperature β into N_t time slices and introduce a spacetime lattice of volume $V_{d+1} \equiv N_t V_d = N_t \times L_s^d$, whose coordinates are labeled by $x = (\ell, \mathbf{x})$ ($\ell = 1, \dots, N_t$). Then, the grand canonical partition function is given as follows (see Ref. [24] for derivation):

$$Z = \int dA dB e^{-S(A, B)} = \int dA dB e^{-S_0(A, B)} \det D_a(A, B) \det D_b(A, B). \quad (3.7)$$

Here, $A = (A_x)$ and $B = (B_x)$ are scalar fields on the spacetime lattice, and we have introduced $V_{d+1} \times V_{d+1}$ matrices $t = (t_{xy})$ and $\Lambda_0 = ((\Lambda_0)_{xy})$ with indices $x = (\ell, \mathbf{x})$ and $y = (m, \mathbf{y})$ (we reuse the symbol t),

$$t_{xy} \equiv \delta_{\ell m} t_{\mathbf{xy}}, \quad (\Lambda_0)_{xy} \equiv \begin{cases} \delta_{\ell+1, m} \delta_{\mathbf{xy}} & (\ell < N_t) \\ -\delta_{1, m} \delta_{\mathbf{xy}} & (\ell = N_t). \end{cases} \quad (3.8)$$

Moreover, $S_0(A, B) \equiv (1/2) \sum_x (A_x^2 + B_x^2)$, $h_{a/b} = ((h_{a/b})_x)$ are diagonal matrices with

$$(h_{a/b})_x = e^{\pm(\epsilon \tilde{\mu} + ic_0 A_x) + c_1 B_x - c_1^2}, \quad (3.9)$$

and $D_{a/b}$ are fermion matrices,

$$D_{a/b}(A, B) \equiv h_{a/b} - e^{-\epsilon t} \Lambda_0. \quad (3.10)$$

We employ the symmetric Trotter decomposition, which matches the continuum evolution operator $e^{-\epsilon \hat{H}_\mu}$ up to $O(\epsilon^2)$. Accordingly, we expand $D_{a/b}$ to the same order:³

$$D_{a/b} = h_{a/b} - \Lambda_0 + \epsilon t \Lambda_0 - \frac{\epsilon^2}{2} t^2 \Lambda_0. \quad (3.11)$$

As discussed in Ref. [24], the identity $D_b = D_a^*$ holds at half filling ($\tilde{\mu} = 0$), yielding $\det D_a \det D_b = |\det D_a|^2$. This ensures that the path integral is free from the sign problem at half filling. We expect the sign problem to remain mild when $D_b \approx D_a^*$, which occurs for small α . However, choosing α too small introduces ergodicity issues: zeros of $\det D_{a/b}$ appear on or near the original configuration space Σ_0 , as detailed in Ref. [38]. Thus, there exists an optimal α that mitigates the sign problem on Σ_0 without triggering ergodicity issues.

²The equality directly follows from the identity $(n_{\mathbf{x}}^a + n_{\mathbf{x}}^b - 1)^2 = -(n_{\mathbf{x}}^a - n_{\mathbf{x}}^b)^2 + 1$ (note that $(n_{\mathbf{x}}^{a/b})^2 = n_{\mathbf{x}}^{a/b}$) [38].

³Note that $\Lambda_0 = 1 + O(\epsilon)$ holds only for thermalized configurations and should not be used as a general estimate.

We define the number density operator n and the energy density operator e as follows [24]:

$$n(A, B) \equiv -\frac{1}{V_{d+1}} \left. \frac{\partial S(A, B)}{\partial(\epsilon\mu)} \right|_{\epsilon} + 1 = -\frac{1}{V_{d+1}} \left. \frac{\partial S(A, B)}{\partial(\epsilon\tilde{\mu})} \right|_{\epsilon} + 1, \quad (3.12)$$

$$e(A, B) \equiv \left. \frac{\partial S(A, B)}{\partial\epsilon} \right|_{\epsilon\mu} = \frac{1}{V_{d+1}} \left[\left. \frac{\partial S(A, B)}{\partial\epsilon} \right|_{\epsilon\tilde{\mu}} - \frac{U}{2} \left. \frac{\partial S(A, B)}{\partial(\epsilon\tilde{\mu})} \right|_{\epsilon} \right]. \quad (3.13)$$

Their expectation values can be estimated via the path integral, and are expected to agree with the continuum expectation values of \hat{N}/V_d and \hat{H}/V_d up to $O(\epsilon^2)$ corrections:

$$\langle n \rangle \equiv \frac{1}{V_{d+1}} \frac{\int (dA dB) e^{-S(A, B)} n(A, B)}{\int (dA dB) e^{-S(A, B)}} = \frac{1}{V_d} \frac{\text{tr} e^{-\beta(\hat{H}-\mu\hat{N})} \hat{N}}{\text{tr} e^{-\beta(\hat{H}-\mu\hat{N})}} + O(\epsilon^2), \quad (3.14)$$

$$\langle e \rangle \equiv \frac{1}{V_{d+1}} \frac{\int (dA dB) e^{-S(A, B)} e(A, B)}{\int (dA dB) e^{-S(A, B)}} = \frac{1}{V_d} \frac{\text{tr} e^{-\beta(\hat{H}-\mu\hat{N})} \hat{H}}{\text{tr} e^{-\beta(\hat{H}-\mu\hat{N})}} + O(\epsilon^2). \quad (3.15)$$

4. Setup

We apply WV-HMC to the two-dimensional doped Hubbard model on a lattice of size $L_s \times L_s = 8 \times 8$ with the following parameters: hopping amplitude $t = 1.0$, inverse temperature $\beta = 6.4$, repulsion strength $U = 8.0$ for various values of the chemical potential μ .⁴ The Trotter numbers are $N_t = 24, 22, 20, 18$, corresponding to the Trotter steps $\epsilon = 0.27, 0.29, 0.32, 0.36$. We tune α to the smallest value that avoids ergodicity issues. This allows us to keep the maximum flow time T_1 as small as possible. We choose the upper cutoff T_1 such that the average phase factor on Σ_t , computed using GT-HMC, becomes statistically distinguishable from zero at the two-sigma level at $t \sim T_1$. The weight function parameters [see Eq. (2.8)] are set as follows: $\gamma = 0$, $c_0 = c_1 = 0.01$, and $d_0 = d_1 = 2.0 \times 10^{-3}$.

We perform the simulations using a combined update: two sets of embedded GT-HMC (each trajectory consisting of 25 MD steps with $\Delta s = 4.0 \times 10^{-2}$) followed by one set of pure WV-HMC (each trajectory consisting of 25 MD steps with $\Delta s = 4.0 \times 10^{-4}$). Observables are measured after each combined update, and statistical errors are estimated using the blocked jackknife method.

5. Results

Figure 1 shows the number density as a function of $\tilde{\mu}$ at the Trotter steps $\epsilon = 0.27, 0.29, 0.32$ with β fixed to 6.4. Results obtained using ALF (Algorithm for Lattice Fermions) [39, 40] at $\epsilon = 0.01$ are also shown for comparison. We see that WV-HMC evaluates the number density with controlled statistical errors in a parameter region where the sign problem is serious. We also observe discrepancies between WV-HMC and ALF results in the region $\tilde{\mu} = 5.5\text{--}7.0$, for which the sign problem is not serious and thus the ALF results are reliable.

Figure 2 shows that the number density $\langle n \rangle$ can be fit as $a + b\epsilon^2$ for the results at $\epsilon = 0.27, 0.29, 0.32$ (as well as the result at $\epsilon = 0.36$ when it is consistent with the linear trend), which agrees with the

⁴In the common notation in condensed matter physics, these parameters correspond to $T/t = 1/(t\beta) = 1/6.4 \approx 0.156$ and $U/t = 8.0$.

expectation from Eqs. (3.14) and (3.15). The energy density $\langle e \rangle$ can also be fit with the same functional form. These fits yield the observables in the continuum limit $\epsilon \rightarrow 0$, which are shown in Fig. 3. We find that WV-HMC yields observables with controlled statistical errors even in the continuum limit. The discrepancies between WV-HMC and ALF results observed at finite ϵ indeed disappear in the continuum limit.

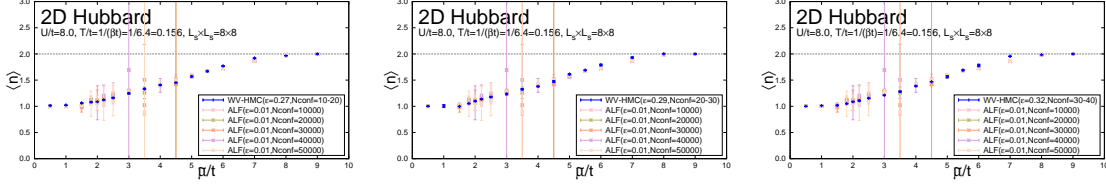


Figure 1: The number density $\langle n \rangle$ at $\epsilon = 0.27, 0.29, 0.32$, compared with results using ALF at $\epsilon = 0.01$.

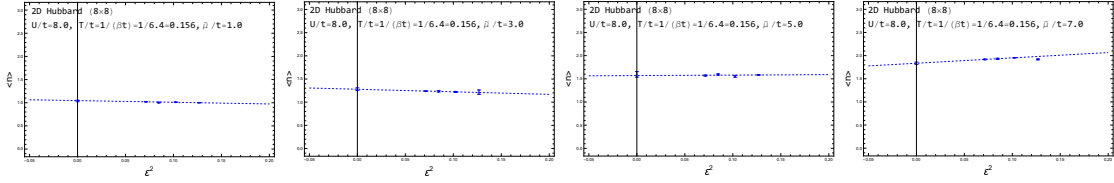


Figure 2: Finite- ϵ effects in the number density $\langle n \rangle$ for $\tilde{\mu} = 1.0, 3.0, 5.0, 7.0$ (figure adapted from [25]).

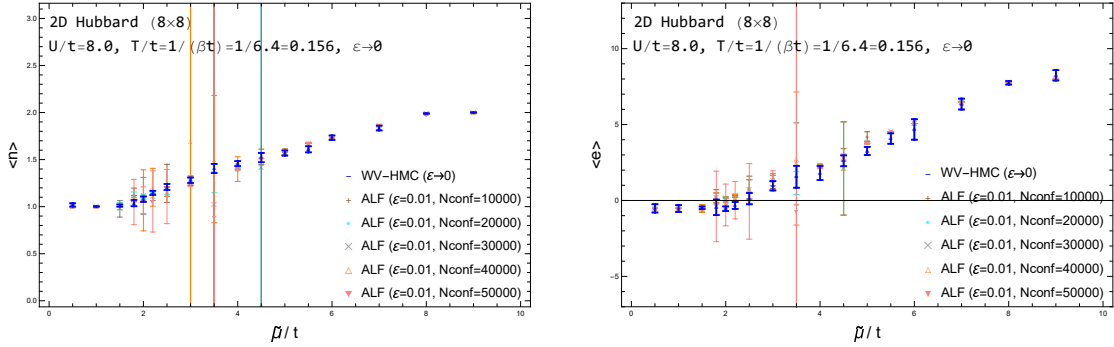


Figure 3: Number density $\langle n \rangle$ and energy density $\langle e \rangle$ in the continuum limit $\epsilon \rightarrow 0$, compared with results using ALF at $\epsilon = 0.01$ (figure adapted from [25]).

6. Conclusion

We applied WV-HMC to the two-dimensional doped Hubbard model on an 8×8 lattice at $T/t = 1/6.4 \simeq 0.156$ and $U/t = 8.0$. The tuning of α mitigates the sign problem on the original integration surface, allowing the maximum flow time T_1 to be significantly reduced. Although this introduces an ergodicity issue for a thin layer of WV-HMC, the problem is successfully resolved by embedding GT-HMC into the process. Using this combined algorithm, we took the continuum

limit in the temporal direction ($\epsilon \rightarrow 0$) and demonstrated that observables can be evaluated with controlled statistical errors. The techniques developed here are expected to scale for the Hubbard model on larger lattices, which we are currently investigating.

Acknowledgments

The authors thank Sinya Aoki, Fakher F. Assaad, Masatoshi Imada, Ken-Ichi Ishikawa, Issaku Kanamori, Yoshio Kikukawa, Nobuyuki Matsumoto, Yusuke Nomura, Maksim Ulybyshev, Youhei Yamaji, and Shiwei Zhang for valuable discussions. This work was partially supported by JSPS KAKENHI Grant Numbers JP20H01900, JP21K03553, JP23H00112, JP23H04506, JP24K07052; by MEXT as "Program for Promoting Researches on the Supercomputer Fugaku" (Simulation for basic science: approaching the new quantum era, JPMXP1020230411); by SPIRIT2 2025 of Kyoto University. We used computational resources of the supercomputer Fugaku provided by the RIKEN Center for Computational Science (Project ID: hp230207, hp240213).

References

- [1] H. Yokoyama and H. Shiba, *Variational monte-carlo studies of hubbard model. i*, *Journal of the Physical Society of Japan* **56** (1987) 1490.
- [2] K. Yamaji, T. Yanagisawa, T. Nakanishi and S. Koike, *Variational monte carlo study on the superconductivity in the two-dimensional hubbard model*, *Physica C: Superconductivity* **304** (1998) 225–238.
- [3] S. Sorella, *Wave function optimization in the variational monte carlo method*, *Physical Review B* **71** (2005) .
- [4] D. Tahara and M. Imada, *Variational monte carlo method combined with quantum-number projection and multi-variable optimization*, *Journal of the Physical Society of Japan* **77** (2008) 114701.
- [5] S. Zhang, J. Carlson and J.E. Gubernatis, *Constrained Path Quantum Monte Carlo Method for Fermion Ground States*, *Phys. Rev. Lett.* **74** (1995) 3652 [cond-mat/9503055].
- [6] S. Zhang, J. Carlson and J.E. Gubernatis, *A Constrained path Monte Carlo method for fermion ground states*, *Phys. Rev. B* **55** (1997) 7464 [cond-mat/9607062].
- [7] A. Mukherjee and M. Cristoforetti, *Lefschetz thimble Monte Carlo for many-body theories: A Hubbard model study*, *Phys. Rev. B* **90** (2014) 035134 [1403.5680].
- [8] M.V. Ulybyshev and S.N. Valgushev, *Path integral representation for the Hubbard model with reduced number of Lefschetz thimbles*, 1712.02188.
- [9] M. Ulybyshev, C. Winterowd and S. Zafeiropoulos, *Taming the sign problem of the finite density Hubbard model via Lefschetz thimbles*, 1906.02726.

- [10] M. Ulybyshev, C. Winterowd and S. Zafeiropoulos, *Lefschetz thimbles decomposition for the Hubbard model on the hexagonal lattice*, *Phys. Rev. D* **101** (2020) 014508 [1906.07678].
- [11] M. Ulybyshev, C. Winterowd, F. Assaad and S. Zafeiropoulos, *Instanton gas approach to the Hubbard model*, *Phys. Rev. B* **107** (2023) 045143 [2207.06297].
- [12] M. Ulybyshev and F.F. Assaad, *Beyond the instanton gas approach: dominant thimbles approximation for the Hubbard model*, 2407.09452.
- [13] M. Fukuma, N. Matsumoto and N. Umeda, *Applying the tempered Lefschetz thimble method to the Hubbard model away from half-filling*, *Phys. Rev. D* **100** (2019) 114510 [1906.04243].
- [14] S. Akiyama and Y. Kuramashi, *Tensor renormalization group approach to (1+1)-dimensional Hubbard model*, *Phys. Rev. D* **104** (2021) 014504 [2105.00372].
- [15] S. Akiyama, Y. Kuramashi and T. Yamashita, *Metal–insulator transition in the (2+1)-dimensional Hubbard model with the tensor renormalization group*, *PTEP* **2022** (2022) 023I01 [2109.14149].
- [16] M. Rodekamp, E. Berkowitz, C. Gäntgen, S. Krieg, T. Luu and J. Ostmeier, *Mitigating the Hubbard sign problem with complex-valued neural networks*, *Phys. Rev. B* **106** (2022) 125139 [2203.00390].
- [17] C. Gäntgen, E. Berkowitz, T. Luu, J. Ostmeier and M. Rodekamp, *Fermionic sign problem minimization by constant path integral contour shifts*, *Phys. Rev. B* **109** (2024) 195158 [2307.06785].
- [18] D. Schuh, L. Funcke, J. Kreit, T. Luu and S. Singh, *Tackling the Sign Problem in the Doped Hubbard Model with Normalizing Flows*, 2603.18205.
- [19] M. Fukuma and N. Matsumoto, *Worldvolume approach to the tempered Lefschetz thimble method*, *PTEP* **2021** (2021) 023B08 [2012.08468].
- [20] M. Fukuma, N. Matsumoto and Y. Namekawa, *Statistical analysis method for the worldvolume hybrid Monte Carlo algorithm*, *PTEP* **2021** (2021) 123B02 [2107.06858].
- [21] M. Fukuma, *Simplified Algorithm for the Worldvolume HMC and the Generalized Thimble HMC*, *PTEP* **2024** (2024) 053B02 [2311.10663].
- [22] M. Fukuma, *Worldvolume Hybrid Monte Carlo algorithm for group manifolds*, 2506.12002.
- [23] M. Fukuma and Y. Namekawa, *Applying the Worldvolume Hybrid Monte Carlo method to the two-dimensional Hubbard model*, *PoS LATTICE2024* (2025) 053.
- [24] M. Fukuma and Y. Namekawa, *Applying the Worldvolume Hybrid Monte Carlo method to the Hubbard model away from half filling*, 2507.23748.
- [25] M. Fukuma and Y. Namekawa, *Enhancing the ergodicity of Worldvolume HMC via embedding Generalized-thimble HMC*, 2508.02659.

- [26] E. Witten, *Analytic Continuation Of Chern-Simons Theory*, *AMS/IP Stud. Adv. Math.* **50** (2011) 347 [[1001.2933](#)].
- [27] AURORASCIENCE collaboration, *New approach to the sign problem in quantum field theories: High density QCD on a Lefschetz thimble*, *Phys. Rev. D* **86** (2012) 074506 [[1205.3996](#)].
- [28] M. Cristoforetti, F. Di Renzo, A. Mukherjee and L. Scorzato, *Monte Carlo simulations on the Lefschetz thimble: Taming the sign problem*, *Phys. Rev. D* **88** (2013) 051501 [[1303.7204](#)].
- [29] H. Fujii, D. Honda, M. Kato, Y. Kikukawa, S. Komatsu and T. Sano, *Hybrid Monte Carlo on Lefschetz thimbles - A study of the residual sign problem*, *JHEP* **10** (2013) 147 [[1309.4371](#)].
- [30] H. Fujii, S. Kamata and Y. Kikukawa, *Lefschetz thimble structure in one-dimensional lattice Thirring model at finite density*, *JHEP* **11** (2015) 078 [[1509.08176](#)].
- [31] H. Fujii, S. Kamata and Y. Kikukawa, *Monte Carlo study of Lefschetz thimble structure in one-dimensional Thirring model at finite density*, *JHEP* **12** (2015) 125 [[1509.09141](#)].
- [32] A. Alexandru, G. Basar and P. Bedaque, *Monte Carlo algorithm for simulating fermions on Lefschetz thimbles*, *Phys. Rev. D* **93** (2016) 014504 [[1510.03258](#)].
- [33] A. Alexandru, G. Basar, P.F. Bedaque, G.W. Ridgway and N.C. Warrington, *Sign problem and Monte Carlo calculations beyond Lefschetz thimbles*, *JHEP* **05** (2016) 053 [[1512.08764](#)].
- [34] M. Fukuma and N. Umeda, *Parallel tempering algorithm for integration over Lefschetz thimbles*, *PTEP* **2017** (2017) 073B01 [[1703.00861](#)].
- [35] H.C. Andersen, *RATTLE: A "velocity" version of the SHAKE algorithm for molecular dynamics calculations*, *Journal of Computational Physics* **52** (1983) 24.
- [36] A. Alexandru, *Improved algorithms for generalized thimble method*, talk at the 37th international conference on lattice field theory, Wuhan (2019) .
- [37] M. Fukuma, N. Matsumoto and N. Umeda, *Implementation of the HMC algorithm on the tempered Lefschetz thimble method*, [1912.13303](#).
- [38] S. Beyl, F. Goth and F.F. Assaad, *Revisiting the Hybrid Quantum Monte Carlo Method for Hubbard and Electron-Phonon Models*, *Phys. Rev. B* **97** (2018) 085144 [[1708.03661](#)].
- [39] M. Bercx, F. Goth, J.S. Hofmann and F.F. Assaad, *The ALF (Algorithms for Lattice Fermions) project release 1.0. Documentation for the auxiliary field quantum Monte Carlo code*, *SciPost Phys.* **3** (2017) 013 [[1704.00131](#)].
- [40] ALF collaboration, *The ALF (Algorithms for Lattice Fermions) project release 2.4. Documentation for the auxiliary-field quantum Monte Carlo code*, *SciPost Phys. Codeb.* **2022** (2022) 1 [[2012.11914](#)].